

DESY-03-181
HU-EP-03/74
SFB/CPP-03-46

Axial Correlation Functions in the ϵ -Regime: a Numerical Study with Overlap Fermions

W. Bietenholz^a, T. Chiarappa^b, K. Jansen^b,
K.-I. Nagai^b and S. Shcheredin^a

^a Institut für Physik, Humboldt Universität zu Berlin
Newtonstr. 15, D-12489 Berlin, Germany

^b NIC/DESY Zeuthen
Platanenallee 6, D-15738 Zeuthen, Germany

We present simulation results employing overlap fermions for the axial correlation functions in the ϵ -regime of chiral perturbation theory. In this regime, finite size effects and topology play a dominant rôle. Their description by quenched chiral perturbation theory is compared to our numerical results in quenched QCD. We show that lattices with a linear extent $L > 1.1$ fm are necessary to interpret the numerical data obtained in distinct topological sectors in terms of the ϵ -expansion. Such lattices are, however, still substantially smaller than the ones needed in standard chiral perturbation theory. However, we also observe severe difficulties at very low values of the quark mass, in particular in the topologically trivial sector.

1 Introduction

There are a number of questions in QCD where lattice simulations are hardly feasible in the physical regime, e.g., when the light quark masses assume their physical values and the physical volume is large enough to accommodate the light mesons. However, in some occasions it is possible to extract physical information from simulation results obtained in an *unphysical* setup, in particular in an unphysically small volume. The variation of the volume then allows for the investigation of finite size effects (FSE), which provide information about the same system in a large volume. Examples for this strategy are the non-perturbative renormalization procedure based on the Schrödinger Functional [1] and the evaluation of a scattering length based on the analysis of the level repulsion [2]. A further example — which will be discussed here — is the study of the dynamics of quasi-Goldstone bosons in the ϵ -regime of chiral perturbation theory (χ PT).

One procedure to make use of the FSE is the transmutation of the variation of the volume into a variation of the physical scale. Then the effect on certain scale-dependent observables enables for instance the determination of a running coupling constant [3].

An alternative procedure — that we are going to deal with — is based on the fact that even in small volumes the FSE are characterized by *infinite volume parameters*. Therefore the evaluation of FSE provides access to physical quantities. That situation occurs in particular in a specific regime of χ PT, where the pion Compton wave length is much larger than the linear extent of the volume, while the inverse linear extent is far below the QCD cutoff scale. The resulting FSE are described in χ PT — which considers the pions as quasi-Goldstone bosons of the chiral symmetry breaking — by the so-called ϵ -expansion [4]. The corresponding zero-modes are treated exactly by means of collective variables, while the non-zero modes, as well as the pion mass, are dealt with perturbatively; note that the fluctuations around the zero modes do fit into the box. The domain where this expansion applies is denoted as the ϵ -regime.

As a test case for QCD, the ϵ -expansion can also be applied to the $O(N)$ symmetric linear [5] and non-linear [6] σ -model. For the case of the 4d $O(4)$ model the numerical technique of extracting infinite volume parameters from FSE was applied very successfully [7]. In QCD such theoretical concepts are often tested in the quenched approximation where simulations are much

easier, although the concept is designed for full QCD. It turned out that quenched results are quite often close to experimental quantities [8], even though there is no reason to expect this behavior in general. At low energy, it is important that also *quenched* χPT has been worked out [9, 10, 11], hence quenched QCD can be used to probe the applicability of this procedure. This is the motivation for our pilot study, which has the purpose to gain first experience on

- the range for the physical volume where the ϵ -expansion is applicable
- the extent of the statistics which is required for reliable results in this framework
- the sources of potential difficulties, and their dependence on the topological sector.

Our statistics is rather modest and it should be enlarged for precise results. We hope, however, to provide a sound basis for the prospects of simulations in the ϵ -regime, also in view of full QCD.

So far the ϵ -regime appeared as a *terra incognita* for numerical studies of QCD because until recently no formulation of lattice fermions was known which would be suitable in this context. The obstacles for such a formulation are linked to the problems in formulating chiral symmetry and topological charges ν on the lattice — note that topology becomes extremely important for χPT in small volumes [12]. None of these problems is solved by the Wilson fermion, and at small quark masses the latter also runs into technical problems such as the significance of exceptional configurations. The staggered fermion, on the other hand, seems to be “topology blind”, i.e. its results do not depend on ν — at least not for strong and moderate gauge couplings, which were tested so far — in contrast to the continuum [13].¹

A solution to these two problems is now available due to the recent formulation of chirally invariant lattice fermions. Their Dirac operator obeys the Ginsparg-Wilson relation [15] and an operator of that kind will be used in this work. However, its application is very computation time demanding, hence its use in QCD is restricted to the quenched approximation at

¹Using very smooth gauge fields and smeared links, topological structures can be seen by the staggered fermion, as a very recent study shows in the Schwinger model [14].

present and in the foreseeable future. For domain wall fermions as another realization of a Dirac operator inducing an exact lattice chiral symmetry, an attempt had been made to explore the ϵ -regime [16]. However, the lattices used in that work were unfortunately too small for χ PT to work.

In Section 2 we describe the lattice formulation of our simulations and the formulae of quenched χ PT which are relevant in this context. In Section 3 our numerical results for the axial correlation functions in distinct topological sectors are compared to the predictions of quenched χ PT. We also discuss the stability of such numerical results, which is most problematic in the topologically trivial sector. Section 4 is devoted to our conclusions and to an outlook on this new field of research. A synopsis of our results was given in Refs. [17, 18].

2 Chiral invariant lattice fermions and chiral perturbation theory

2.1 Overlap fermions

The lattice Dirac operator that we are going to use is the so-called overlap operator [19]. On a lattice of unit spacing the massless operator is given by

$$D_{\text{ov}}^{(0)} = \mu \left[1 + A / \sqrt{A^\dagger A} \right] , \quad A = D_W - \mu , \quad (2.1)$$

where D_W is the Wilson-Dirac operator (with Wilson parameter 1 and $\kappa = 1/8$), and μ is a mass parameter, which can be chosen in some interval that shrinks as the gauge coupling increases. Our simulations were performed at $\beta = 6$ and we set $\mu = 1.4$, which is optimal for locality in this case [20]. This observation referred to the Wilson gauge action that we were also using throughout this work.

$D_{\text{ov}}^{(0)}$ is a solution to the Ginsparg-Wilson relation [15]

$$D_{\text{ov}}^{(0)} \gamma_5 + \gamma_5 D_{\text{ov}}^{(0)} = \frac{1}{\mu} D_{\text{ov}}^{(0)} \gamma_5 D_{\text{ov}}^{(0)} , \quad (2.2)$$

which excludes additive mass renormalization and exceptional configurations. Hence $D_{\text{ov}}^{(0)}$ has exact zero modes with a definite chirality [21]. This provides

a sound definition of the topological charge of a lattice gauge configuration by means of the Atiyah-Singer Index Theorem. These amazing properties are related to the fact that Ginsparg-Wilson fermions have an exact lattice chiral symmetry [22], which turns into the standard chiral symmetry in the continuum limit.

For practical applications we still have to insert a small bare quark mass m_q . It is added to $D_{\text{ov}}^{(0)}$ as follows,

$$D_{\text{ov}} = \left(1 - \frac{m_q}{2\mu}\right) D_{\text{ov}}^{(0)} + m_q . \quad (2.3)$$

The challenge to numerical studies is the inverse square root in eq. (2.1). It is basically equivalent — but somewhat more convenient — to evaluate the sign function of the Hermitian operator $\gamma_5 A$. In our simulations we approximated this sign function by Chebyshev polynomials to an accuracy of 10^{-12} for the eigenvalues and 10^{-16} for the propagators. For the description of highly optimized algorithmic tools to deal with overlap fermions we refer to Refs. [23, 24].

2.2 The ϵ -regime in quenched chiral perturbation theory

The low energy properties of QCD can be described by an effective Lagrangian \mathcal{L}_{eff} , and χ PT is a powerful tool for its construction and evaluation [25]. At leading order, \mathcal{L}_{eff} is parametrized by the pion decay constant F_π and the scalar condensate Σ ,

$$\mathcal{L}_{\text{eff}}[U] = \frac{F_\pi^2}{4} \text{Tr}[\partial_\mu U \partial_\mu U^\dagger] - \frac{1}{2} \Sigma m_q \text{Tr}[U e^{i\theta/N_f} + U^\dagger e^{-i\theta/N_f}] , \quad (2.4)$$

where $U(x) \in SU(N_f)$ is the quasi-Goldstone boson field, N_f is the number of quark flavors and θ the vacuum angle. (For simplicity we assume a single bare mass m_q for all flavors.) Note that the values of F_π and Σ in a finite volume and in infinite volume coincide, up to logarithmic corrections which are specific to the quenched approximation.

Depending on the counting rules for the expansion, one distinguishes two regimes for the χ PT: the “ p -expansion” applies to large volumes where FSE are suppressed [26], which is the standard situation. In contrast, the “ ϵ -expansion” assumes a very small quark mass — even below the physical

masses of the u and d quarks — so that $m_\pi L \ll 1$, where $m_\pi \propto \sqrt{m_q}$ is the pion mass and L is the linear size of the system. In this regime FSE are strong, but they can be described analytically for dynamical as well as quenched quarks [4, 9, 10]. As an important feature, the observables depend significantly on the topology [12], hence they should be measured by averages over gauge configurations in a fixed topological sector (or, more precisely, at a fixed absolute value of the topological charge ν). In the light of the requirements of small quark masses and a well-defined topology, the use of Ginsparg-Wilson fermions is ideal, as we pointed out before.

In this work we aim at a first interpretation of lattice data — obtained from simulating overlap fermions — in the framework of the ϵ -expansion. In particular, our reference point is the formula for the axial correlation function in quenched χ PT derived in Ref. [10]. Using this formula, the lattice data yield predictions for the leading (quenched) low energy constants in the effective Lagrangian. In order to stay in the ϵ -regime we have to require the dimensionless scaling variable

$$z = m_q \Sigma V \quad (2.5)$$

to be small, i.e. clearly below 1 (where V is the volume).²

To render this paper self-contained we now quote the main result of quenched χ PT which we are going to use in our data analysis. This result was obtained [10] consistently from two different methods called “supersymmetric” [27] and “replica” [28]. Ref. [10] also showed that the corresponding vector correlation function vanishes to all orders in the quenched ϵ -expansion; a general argument is added in Ref. [29].

We start from the definition of the bare axial current at momentum $\vec{p} = \vec{0}$ and Euclidean time t ,

$$A_\mu(t) = \sum_{\vec{x}} \bar{\psi}(t, \vec{x}) \gamma_5 \gamma_\mu \psi(t, \vec{x}) . \quad (2.6)$$

The formula for the axial correlation function in a volume $L^3 \times T$, to the first

²If we insert $\Sigma = (250 \text{ MeV})^3$ as a typical value from the literature, the parameters of our results in Figs. 3 to 6 correspond to $z \simeq 0.34$.

order in quenched χ PT, reads³

$$\begin{aligned}\langle A_0(t) A_0(0) \rangle_\nu &= 2 \cdot \left(\frac{F_\pi^2}{T} + 2m_q \Sigma_{|\nu|}(z) T \cdot h_1(\tau) \right), \\ h_1(\tau) &= \frac{1}{2} \left(\tau^2 - \tau + \frac{1}{6} \right), \quad \tau = \frac{t}{T}, \\ \Sigma_\nu(z) &= \Sigma \left(z \left[I_\nu(z) K_\nu(z) + I_{\nu+1}(z) K_{\nu-1}(z) \right] + \frac{\nu}{z} \right).\end{aligned}\tag{2.7}$$

I_ν and K_ν are modified Bessel functions, z is defined in eq. (2.5), ν is again the topological charge, and h_1 is a purely kinematic function. The latter shows that this correlation function is given by a parabola in t with its minimum at $T/2$. This behavior is qualitatively different from the infinite volume, where the correlations decay exponentially (resp. as a `cosh` function in a periodic volume). However, the small and the infinite volume have in common that in both cases the quenched axial correlation function to the first order only depends on the coupling constants F_π and Σ . In contrast, the quenched pseudoscalar-pseudoscalar and the scalar-scalar correlation functions involve further parameters [9], which motivated our focus on the simple case of the axial correlation function (2.7). We note that the bare axial current in eq. (2.6) needs to be renormalized multiplicatively by applying a renormalization constant Z_A , see below.

At this point we would like to mention that Random Matrix Theory can be applied to QCD [30], also in the quenched case [31]. Random Matrix Theory involves additional assumptions and it leads to explicit predictions for the distributions of the low lying eigenvalues of the Dirac operator [32]. If these predictions hold, they provide another way to extract values for Σ and (somewhat more involved) for F_π from lattice data. In recent studies of the spectrum of $D_{\text{ov}}^{(0)}$ it turned out that these Random Matrix predictions are essentially confirmed, *if* the volume is not too small, which means for the linear size: $L \gtrsim 1.2$ fm [33]. This agrees roughly with an earlier study using a truncated fixed point action on a 4^4 lattice [34]. Proceeding to larger physical volumes the quality of the agreement with the Random Matrix prediction improves further [35].

In particular the probability distribution for the first non-zero Dirac eigenvalue $|\lambda_1|$ has a peak, which moves to larger values (of $|\lambda_1|V\Sigma$) as $|\nu|$ in-

³We have an extra factor of 2 compared to Ref. [10] because our definition of the current does not involve flavor space generators.

lattice size	complete statistics	number of configurations		
		$\nu = 0$	$ \nu = 1$	$ \nu = 2$
$10^3 \times 24$	65	20	24	17
12^4	157	47	78	24

Table 1: *The statistics of our simulations on two lattices, which we simulated both at $\beta = 6$.*

creases, where ν is the topological charge. In the neutral sector, $\nu = 0$, there is a significant density of very small eigenvalues. A previous study of the chiral condensate [36] observed that this property yields severe problems for measurements in the sector $\nu = 0$. That observation was confirmed in a striking way by our investigation that we are going to present in the next Section.

3 Numerical results

In our simulations we used the overlap operator D_{ov} described in Subsection 2.1. We simulated quenched QCD on periodic lattices of two sizes, $10^3 \times 24$ and 12^4 , both at $\beta = 6$. This corresponds to physical volumes of $(0.93 \text{ fm})^3 \times 1.86 \text{ fm}$ resp. $(1.12 \text{ fm})^4$.⁴

To determine the topological charge we computed the index, i.e. the difference between the number of right-handed and left-handed zero modes of $D_{\text{ov}}^{(0)}$, by using either the Ritz functional method [38] or the Arnoldi procedure [39]. We mention in passing that the index was always given by the number of zero modes with only one chirality; we never encountered zero modes of opposite chiralities in the same configuration, as it is expected in general for interacting chiral fermions [24, 40].

Our statistics on the two lattice sizes is given in Table 1. On such small volumes most configurations have charges $|\nu| \leq 2$, and we have the largest statistics at $|\nu| = 1$.

⁴Our physical scale is based on the Sommer parameter [37]. In the following we do not keep track of possible errors in that scale.

The parameter F_π is determined through the minimum of the function in eq. (2.7) at $\tau = 1/2$ and it is hence easy to fit. Σ , on the other hand, is related to the curvature of the predicted parabola and more difficult to extract, as we are going to see.⁵

First we observed also here that the physical volume must exceed the lower limit mentioned in Subsection 2.2. As a striking example, we show that otherwise one does not obtain the curvature required at $|\nu| = 1$ by any positive value of Σ . This is illustrated in Fig. 1 (on the right), where our data from the $10^3 \times 24$ lattice are shown, as well as the analytic curves given by eq. (2.7) for $\Sigma = 0$ and $\Sigma = (250 \text{ MeV})^3$. The fact that those two curves can hardly be distinguished is typical for all sectors with $\nu \neq 0$, due to the last term in the expression of eq. (2.7) for Σ_ν .

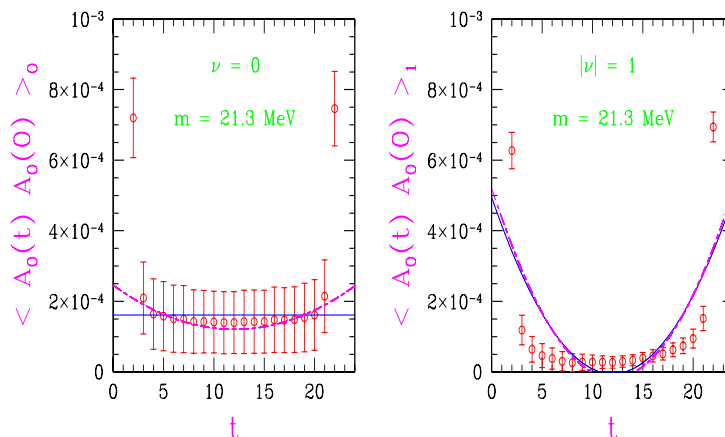


Figure 1: Data for the axial correlation function from a $10^3 \times 24$ lattice at $\beta = 6$. For comparison we also show the curves predicted by quenched χPT for $\Sigma = 0$ (solid line) and $\Sigma = (250 \text{ MeV})^3$ (dashed line). The plot for $|\nu| = 1$ (on the right) illustrates clearly that the lattice size chosen here is not compatible with χPT , as it could be expected also based on the comparison to Random Matrix Theory [33].

Once we are in the ϵ -regime, $\nu = 0$ may look like the most convenient case from eq. (2.7). In particular this is the only sector which does not have

⁵This situation is somehow complementary to the comparison of the eigenvalue distributions to their Random Matrix predictions, where Σ is easier to determine.

the problem of the tiny sensitivity of the predicted function on the value of Σ , see Fig. 1 on the left. Unfortunately, from the numerical point of view this sector is a nightmare. Its problems are related to the danger of very small eigenvalues, as we mentioned in Subsection 2.2. This causes the large error bars in Fig. 1 on the left. To illustrate this problem explicitly we show in Fig. 2 the histories for our measurements of $\langle A_0(t) A_0(0) \rangle_0$ and $\langle A_0(t) A_0(0) \rangle_1$. In the topologically neutral sector there are strong spikes. We checked that these spikes appear exactly at those configurations which have very small eigenvalues. The height of the spikes is maximal at very small bare quark mass m_q , as Fig. 3 shows.⁶ In the chiral limit $m_q \rightarrow 0$ the spike height is proportional to $1/|\lambda_1|$. Qualitatively this property also holds for the (smaller) spikes in the non-trivial sectors, where, however, the occurrence of such very small modes is suppressed; this suppression gets stronger for increasing values of $|\nu|$. Therefore we have some kind of a tuning problem for m_q : on one hand it must be very small to make sure we are in the ϵ -regime, but on the other hand taking it too small makes measurements statistically tedious, in addition to numerical problems when evaluating the propagators (c.f. footnote 6).

Returning to $m_q = 21.3$ MeV, we would now like to get an idea of the effect of such spikes, i.e. we want to estimate how many configurations would be required to obtain stable expectation values. For this purpose we consider the contribution of the smallest (non-zero) eigenvalue λ_1 alone to the scalar condensate. This contribution reads

$$\Sigma_{\min}^{(\nu)} = \frac{1}{V} \int_0^\infty dz_1 P_\nu(z_1) \frac{2m_q}{m_q^2 + (z_1/\Sigma V)^2}, \quad z_1 = \lambda_1 \Sigma V, \quad (3.1)$$

where we insert the probabilities $P_\nu(z_1)$ provided by Random Matrix Theory [32]. We generated fake numbers for the lowest eigenvalue with probability $P_\nu(z_1)$ and computed $\Sigma_{\min}^{(\nu)}$ from them. The result can only be trusted when the standard deviation becomes practically constant. Fig. 4 shows the evolution of this standard deviation as the statistics is enhanced. We infer that the sector $\nu = 0$ requires a tremendous statistics of $O(10^4)$ configurations,

⁶Fig. 3 shows data for bare masses in the range of $m_q = 0.2$ MeV \dots 21.3 MeV. The corresponding overlap operators D_{ov} could be inverted simultaneously at all these masses by means of a Multiple Mass Solver. However, if one involves very small masses the latter has a problem of accuracy [41], hence we did not rely on it for our results at $m_q = 21.3$ MeV and used standard inverters at this single mass only.

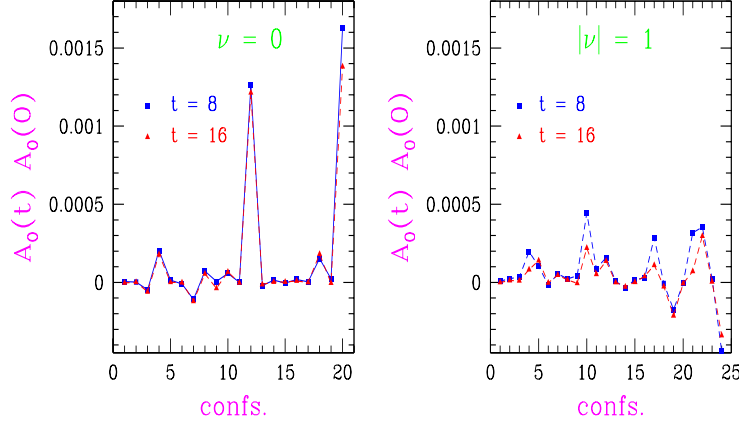


Figure 2: *Histories of the axial correlation function $A_0(t)A_0(0)$ on a $10^3 \times 24$ lattice at $\beta = 6$ and $m_q = 21.3$ MeV. We show the histories at $t = 8$ and at $t = 16$. For some $\nu = 0$ configurations (on the left) we recognize marked spikes. At $|\nu| = 1$ (on the right) the history is significantly smoother.*

but the situation is clearly better for $\nu \neq 0$, where $O(100)$ configurations might be sufficient.

We now present our results from the 12^4 lattice, which is close to the point where the applicability of χ PT should set in. The quark mass amounts again to $m_q = 21.3$ MeV.

Fig. 5 (on the left) shows our data for the axial correlation function at $|\nu| = 1$. The curve corresponding to eq. (2.7) can be fitted well over some interval that excludes the points near the boundary (which are strongly affected by the contributions of excited states). This determines the additive constant — and therefore F_π — quite accurately. In Fig. 5 on the right we plot the resulting values of F_π as a function of the number t_f of t values (around $T/2$) that we include in the fit. We find a decent plateau, which suggests a value of $F_\pi = (86.7 \pm 4.0)$ MeV for the quenched, bare pion decay constant. Although the purpose of the present paper is mainly to demonstrate that measurements of $\langle A_0(t)A_0(0) \rangle_{\nu \neq 0}$ do have the potential to determine F_π , let us shortly address the question of renormalization. In principle, the renormalized axial correlation function

$$\langle A_0^R(t)A_0^R(0) \rangle \equiv Z_A^2 \cdot \langle A_0(t)A_0(0) \rangle$$

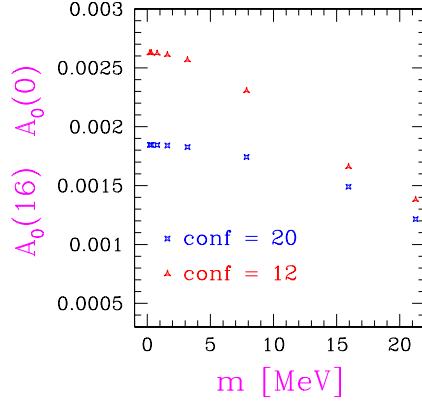


Figure 3: *The height of the two spikes of $A_0(16)A_0(0)$ in the $\nu = 0$ history of Fig. 2, at different quark masses $m_q = 0.2 \text{ MeV} \dots 21.3 \text{ MeV}$.*

has to be considered. As an estimate of the renormalization constant Z_A the value determined in Ref. [42] can be taken which amounts to $Z_A = 1.55$. Thus the value of the pion decay constant as extracted from the bare axial correlation function receives a large renormalization and we find $F_\pi^R \approx 130 \text{ MeV}$. We stress again that the values of F_π and F_π^R computed here are values of the quenched approximation.

The difficulty to extract Σ from our data is illustrated in Fig. 5 (left). It shows fits to $t_f = 7$ points with F_π as a free parameter, for Σ fixed as 0 resp. $(250 \text{ MeV})^3$. Indeed, those two curves can hardly be distinguished.

Finally, as a consistency check we also take a look at charge $|\nu| = 2$. Fig. 6 shows the data and the predicted curve for the parameter range that we extracted before from $|\nu| = 1$. We see that these curves are compatible with our data, within the errors.

4 Conclusions

We presented a pilot study of the axial correlation function — as the simplest example of a meson correlation function — in the ϵ -regime, based on quenched QCD with overlap fermions. We find that there are several conditions for running conclusive simulations with Ginsparg-Wilson fermions in

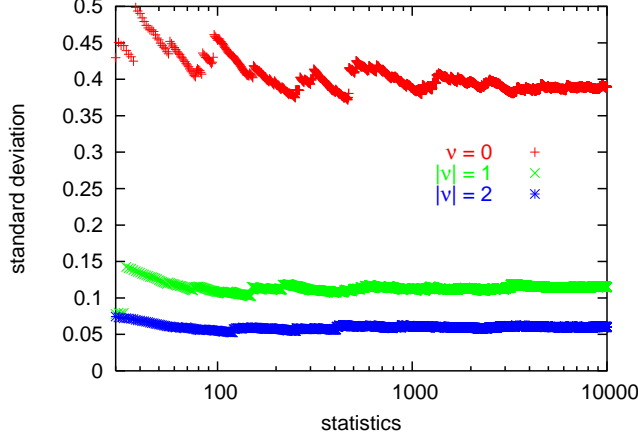


Figure 4: The standard deviation in the (fake) measurement of $\Sigma_{\min}^{(\nu)}$, the contribution of the lowest non-zero eigenvalue to the scalar condensate, given in eq. (3.1). The parameters correspond to a 12^4 lattice at $\beta = 6$ and $m_q = 21.3$ MeV, and we assumed $\Sigma = (250 \text{ MeV})^3$.

the ϵ -regime. The linear size should obey $L \gtrsim 1.1$ fm, and measurements have to be performed in a sector of *non-trivial topology*. The quark mass should be small for conceptual reasons, but taking it too small causes technical problems in the measurements. The above requirement on the linear size is consistent with an earlier observation based on a comparison to the Random Matrix predictions for the eigenvalues [33].

We observed that the neutral sector, $\nu = 0$, is highly unfavorable for measurements, due to the frequent occurrence of very small eigenvalues. The corresponding configurations show marked spikes, which lead to the requirement of a huge statistics of $O(10^4)$ configurations.

Therefore we worked in the sectors $|\nu| = 1$ and 2. Although our statistics is still rather modest, we recognize that the data *can* be fitted to the functions predicted by quenched χ PT. These fits allow for a stable determination of the quenched value of F_π . With our present analysis we were not able to determine Σ since large variations of this parameter hardly changes the fit to the axial correlation function. The only exception is the sector $\nu = 0$, see Fig. 1. However, exactly there the statistical results are ruined by strong spikes, as we pointed out before.

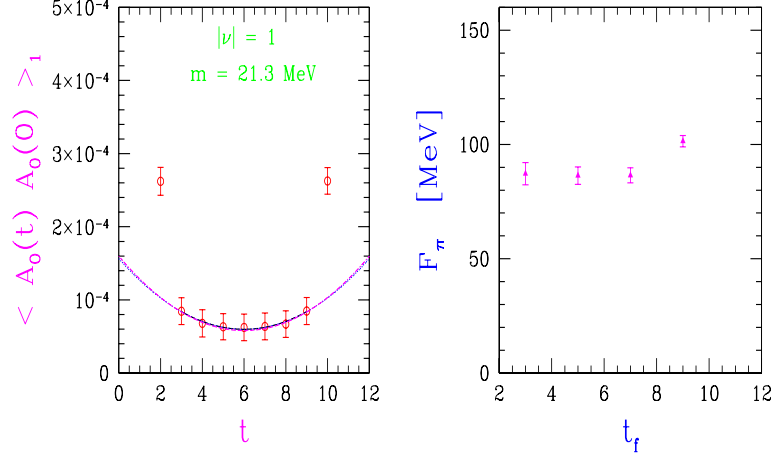


Figure 5: *The axial correlation function on a 12^4 lattice at $\beta = 6$ in the sector $|\nu| = 1$ (on the left). The two lines — which are hardly distinguishable in this plot — are fits of the curve predicted by quenched χ PT with the free parameter F_π and $\Sigma = 0$ resp. $(250 \text{ MeV})^3$. On the right we display the values of F_π obtained from fits over t_f points around the center at $t = 6$.*

As an *outlook*, further information could be obtained by considering in addition the pseudoscalar-pseudoscalar and the scalar-scalar correlation function [18]. Then the predictions involve four free parameters, hence it will be more difficult to establish a consistent picture. We also plan to proceed to larger physical volumes where we expect complete agreement with χ PT. In particular, these parameters would then fix directly a one loop approximation to Σ_ν in eq. (2.7), which is also a rough approximation to Σ . We also intend to verify the emerging picture with an alternative Ginsparg-Wilson fermion formulation [43].

The results of this paper suggest that it is advantageous to work in fixed topological sectors with relatively large charges, say $|\nu| = 2 \dots 5$, in order to suppress the effects of low-lying (non-zero) eigenvalues. Hence algorithmic tools or modified gauge actions that would allow for such simulations are highly desirable and should be tested in practice to explore the ϵ -regime.

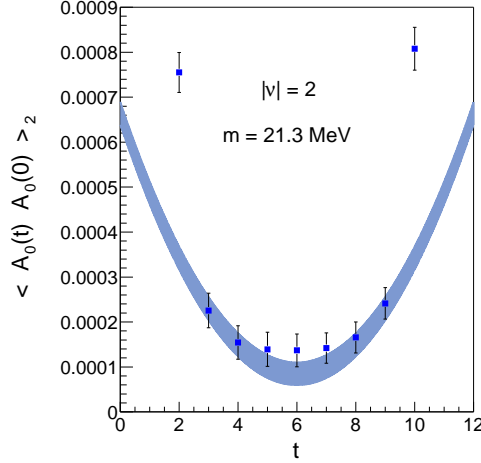


Figure 6: Data from a 12^4 lattice at $\beta = 6$ in the sector $|\nu| = 2$, along with the curves from eq. (2.7). The dark area shows these curves for the parameters in the range that we determined from $|\nu| = 1$. We find agreement with the $|\nu| = 2$ data within the errors.

Acknowledgements We would like to thank Poul Damgaard, Pilar Hernández, Heiri Leutwyler, Martin Lüscher and Rainer Sommer for useful comments. This work was supported by the DFG through the SFB/TR9-03 (Aachen-Berlin-Karlsruhe) and in part by the European Union Improving Human Potential Programme under contracts HPRN-CT-2002-00311 (EURIDICE). We also thank the John von Neumann-Institute for Computing and the Konrad-Zuse-Zentrum for providing the necessary computer resources.

References

- [1] M. Lüscher, R. Narayanan, P. Weisz and U. Wolff, *Nucl. Phys.* **B384** (1992) 168.
M. Lüscher, S. Sint, R. Sommer and P. Weisz, *Nucl. Phys.* **B478** (1996) 365.

- M. Lüscher, S. Sint, R. Sommer, P. Weisz and U. Wolff, *Nucl. Phys.* **B491** (1997) 323.
- [2] M. Lüscher, *Commun. Math. Phys.* **105** (1986) 153.
 - [3] M. Lüscher, P. Weisz and U. Wolff, *Nucl. Phys.* **B359** (1991) 221.
M. Lüscher, R. Sommer, P. Weisz and U. Wolff, *Nucl. Phys.* **B389** (1993) 247; *Nucl. Phys.* **B413** (1994) 481.
 - [4] J. Gasser and H. Leutwyler, *Phys. Lett.* **B188** (1987) 477.
F.C. Hansen, *Nucl. Phys.* **B345** (1990) 685.
F.C. Hansen and H. Leutwyler, *Nucl. Phys.* **B350** (1991) 201.
 - [5] H. Neuberger, *Phys. Rev. Lett.* **60** (1988) 889; *Nucl. Phys.* **B300** (1988) 180.
 - [6] P. Hasenfratz and H. Leutwyler, *Nucl. Phys.* **B343** (1990) 241.
W. Bietenholz, *Helv. Phys. Acta* **66** (1993) 633.
 - [7] A. Hasenfratz, K. Jansen, J. Jersák, C.B. Lang, H. Leutwyler and T. Neuhaus, *Z. Phys.* **C46** (1990) 257.
A. Hasenfratz, K. Jansen, J. Jersák, H.A. Kastrup, C.B. Lang, H. Leutwyler and T. Neuhaus, *Nucl. Phys.* **B356** (1991) 332.
 - [8] T. Yoshié, *Nucl. Phys. B (Proc. Suppl.)* **63A-C** (1998) 3.
 - [9] P.H. Damgaard, M.C. Diamantini, P. Hernández and K. Jansen, *Nucl. Phys.* **B629** (2002) 445.
 - [10] P.H. Damgaard, P. Hernández, K. Jansen, M. Laine and L. Lellouch, *Nucl. Phys.* **B656** (2003) 226.
 - [11] P.H. Damgaard, [hep-lat/0310037](#).
 - [12] H. Leutwyler and A. Smilga, *Phys. Rev.* **D46** (1992) 5607.
 - [13] P.H. Damgaard, U.M. Heller, R. Niclasen and K. Rummukainen, *Nucl. Phys. (Proc. Suppl.)* **83** (2000) 197; *Phys. Rev.* **D61** (2000) 014501.
B.A. Berg, H. Markum, R. Pullirsch and T. Wettig, *Phys. Rev.* **D63** (2001) 014504.

- [14] S. Dürr and C. Hoelbling, [hep-lat/0311002](#).
- [15] P.H. Ginsparg and K.G. Wilson, *Phys. Rev.* **D25** (1982) 2649.
- [16] S. Prelovsek and K. Orginos, *Nucl. Phys. B (Proc. Suppl.)* **119** (2003) 822.
- [17] K.-I. Nagai et al., [hep-lat/0309051](#).
- [18] T. Chiarappa et al., [hep-lat/0309083](#).
- [19] H. Neuberger, *Phys. Lett.* **B417** (1998) 141; *Phys. Lett.* **B427** (1998) 353.
- [20] P. Hernández, K. Jansen and M. Lüscher, *Nucl. Phys.* **B552** (1999) 363.
- [21] P. Hasenfratz, V. Laliena and F. Niedermayer, *Phys. Lett.* **B427** (1998) 125.
P. Hasenfratz, *Nucl. Phys.* **B525** (1998) 401.
- [22] M. Lüscher, *Phys. Lett.* **B428** (1998) 342.
- [23] J. van den Eshof, A. Frommer, Th. Lippert, K. Schilling and H.A. van der Vorst, *Comput. Phys. Commun.* **146** (2002) 203.
- [24] L. Giusti, C. Hoelbling, M. Lüscher and H. Wittig, *Comput. Phys. Commun.* **153** (2003) 31.
- [25] J. Gasser and H. Leutwyler, *Annals Phys.* **158** (1984) 142; *Nucl. Phys.* **B250** (1985) 465.
- [26] J. Gasser and H. Leutwyler, *Phys. Lett.* **B184** (1987) 83.
- [27] A. Morel, *J. Physique* **48** (1987) 1111.
C. Bernard and M. Golterman, *Phys. Rev.* **D46** (1992) 853.
- [28] P.H. Damgaard and K. Splittorff, *Phys. Rev.* **D62** (2000) 54509.
- [29] P.H. Damgaard, P. Hernández, K. Jansen, M. Laine and L. Lellouch, [hep-lat/0309015](#).

- [30] J.C. Osborn, D. Toublan and J.J.M. Verbaarschot, *Nucl. Phys.* **B540** (1999) 317.
- [31] P.H. Damgaard, *Nucl. Phys.* **B608** (2001) 162.
- [32] P.H. Damgaard and S.M. Nishigaki, *Nucl. Phys.* **B518** (1998) 495; *Phys. Rev.* **D63** (2001) 045012.
T. Wilke, T. Guhr and T. Wettig, *Phys. Rev.* **D57** (1998) 6486.
S.M. Nishigaki, P.H. Damgaard and T. Wettig, *Phys. Rev.* **D58** (1998) 087704.
- [33] W. Bietenholz, K. Jansen and S. Shcheredin, *JHEP* **07** (2003) 033.
- [34] P. Hasenfratz, S. Hauswirth, T. Jörg, F. Niedermayer and K. Holland, *Nucl. Phys.* **B643** (2002) 280.
- [35] L. Giusti, M. Lüscher, P. Weisz and H. Wittig, [hep-lat/0309189](#).
D. Galletly et al., [hep-lat/0310028](#).
- [36] P. Hernández, K. Jansen and L. Lellouch, *Phys. Lett.* **B469** (1999) 198.
- [37] M. Guagnelli, R. Sommer and H. Wittig, *Nucl. Phys.* **B535** (1998) 389.
- [38] B. Bunk, K. Jansen, M. Lüscher and H. Simma, DESY report (September 1994).
T. Kalkreuter and H. Simma, *Comput. Phys. Commun.* **93** (1996) 33.
- [39] C. Lanczos, *J. Res. Nat. Bur. Stand.* **49** (1952) 33.
D.C. Sorensen, *Siam J. Matrix Anal. Appl.* **13** (1992) 357.
- [40] M. Lüscher, private communication.
- [41] P. Hernández, private communication.
- [42] F. Berruto, N. Garron, C. Hoelbling, L. Lellouch, C. Rebbi and N. Shores, [hep-lat/0310006](#).
- [43] W. Bietenholz, *Nucl. Phys.* **B644** (2002) 223.